Estimation of Melting Layer Altitudes from Dual-Polarization Weather Radar Observations

Reino Keränen[1], Laura Catalina Alku[1,2], Jason Selzler[3]

[1]*Vaisala Oyj. Vanha Nurmijärventie 21. 01670 Vantaa, Finland*
[2]*Helsinki University. Erik Palmenin Aukio 1. 00014 University of Helsinki, Finland*
[3]*Vaisala Inc.3 Lan Drive Suite 100, Westford, MA 01886, USA*

(Dated: 29 August 2014)

1 Introduction

The melting layer (ML) is a significant phenomenon in weather radar observations. It consists of initially frozen hydrometeors falling into air below the 0°C isotherm (freezing level) where they start melting. The radar echoes from melting hydrometeors differ from those from rain droplets as well as from frozen hydrometeors, and ML is observed as the radar bright band. The ML is a complex atmospheric process and rich with features, while the operational weather radar often observes ML in the coarse view. The presence of bright band needs to be accounted for in the quantitative interpretations of weather radar observations. In operational uses, the height of ML (MLHGT) is a primary parameter of the ML feature. The apparent thickness of the bright band is typically a convolution of the actual ML depth and the radar beam. MLHGT can be defined as the altitude of ML top with respect to the mean sea level.

MLHGT is a parameter in many radar data algorithms, such as the estimates of surface rainfall intensity and as the distinctions of convective and stratiform precipitation types. In general, MLHGT can be inferred or needs to be known, when the precipitation is modeled in terms of vertical profiles in the atmosphere (Koistinen and Pohjola, 2014). MLHGT indicates the domains of attenuation induced by various types of precipitation. MLHGT is a key constraint in identification of hydrometeors by dual-polarization which is ambiguous between light rain and snow crystals. In simplest constructions, these methods insist on a unique value of MLHGT i.e. an unambiguous ML is assumed to exist. The 0°C isotherm can be used as a proxy of MLHGT.

In reality, ML is characterized by large temporal and spatial variability (Fabry and Zawadzki, 1995). A smooth ML is a feature of stratiform precipitation, while complicated structures of ML develop in convection of various scales and daily observations indicate they are possible in frontal systems, too. ML may be absent in cool season precipitation and in specific types of warm rain. The 0°C isotherm varies in the large spatial and temporal scale, in particular in the climates of mid-latitudes characterized by fast changing synoptic weather as well as by distinct seasons. The 0°C isotherm is seasonally nearly a constant in parts of tropics. Given the large variability of MLHGT in the temporal and spatial scales typical in weather radar observations, the regional climatological mean values of the 0°C isotherm are coarse approximations of MLHGT. External synoptic observations or predictions derived from numerical models provide more precise information, albeit often with latency or with uncertainty.

In the view point of typical operational uses, we have implemented a method for estimating variable fields of MLHGT to be utilized in the radar signal and data processing. The mapping method is primarily based on the known capability of dual-polarization weather radar to recognize melting snow. We consider observations available in the mode of simultaneous transmission and reception (STAR). A Bayesian approach combines the locations of recognized melting snow and of other type of precipitation in operational volume scans. The radar observations sample the melting layer at a high resolution close to the radar while the resolution degrades in observations at distances beyond 100 km which are still useful in favorable conditions. The method is designed to consider all the sweep data including the lowest elevation PPI scans. RHI scans are combined, when available in the radar data. Information cumulates from consecutive volumes scanned by the radar. They are consistently integrated with the external information of the climatological or synoptic 0°C isotherms when radar observations are lacking. This approach guarantees that the MLHGT estimates are available at all times and at all radar distances in the single data source formatted as the MLHGT map products. At the same time, the MLHGT maps allow reporting the spatial and temporal variability of ML at the finest resolution of the weather radar when observations of precipitation are available. We choose not to extrapolate the detailed features observed close to the radar to estimate MLHGT at far distances. Consistent models of uncertainty and of radar data confidence are essential MLHGT product elements which enable automated interpretation of the information in multiple applications and use cases.

We first brief out generally known features of melting layer in the view point of weather radar and some methods of melting layer recognition. We describe the main building blocks of the proposed MLHGT method and illustrate its key capabilities, with examples of data acquired by the Vaisala WRM200 and WRK200 C-band weather radars which are operated concurrently in the Helsinki area in Finland. We have carried out initial validation of the MLHGT estimates in warm and in cool seasons, through a comparison with 0°C isotherms retrieved from the upper air soundings launched within the radar range.

2 Melting layer

A comprehensive description of the radar observations of ML involves with coupled models of atmospheric dynamics and of microphysics (Szyrmer, Zawadzki, 1999), with general electromagnetic properties of melting hydrometeors (Fabry, Szyrmer, 1999), and with refined details in their inner structure (Zawadzki et al, 2005). A bulk parameterization has been derived of the reflectivity profiles with bright band, applicable to midlatitudes stratiform precipitation (Heyrath et al, 2008). Heyrath et al. (2008) conclude the reflectivity bright band is primarily the effect higher di-electric constant of water compared to that of ice, which implies increased back-scatter cross-section of melting hydrometeors. The hydrometeor shapes and their density play a non-negligible role.

Further features of ML are evident in the dual-polarization radar quantities. The typically utilized signatures of the bright band are: vertical gradients in reflectivity (Z) and in differential reflectivity (Z_{dr}), increased values of Z_{dr} from the expectation from light rain, reduced values of the magnitude of the correlation coefficient between H and V channel echo ($|\rho_{hv}|$) from the expectations from rain and ice crystals. Figure 1 illustrates an example of the dual-polarization signatures of bright band in observations of C-band dual-polarization Doppler radar. In an event of wide spread precipitation, the bright band is unambiguous in each field of Z, of $|\rho_{hv}|$ and of Z_{dr}.

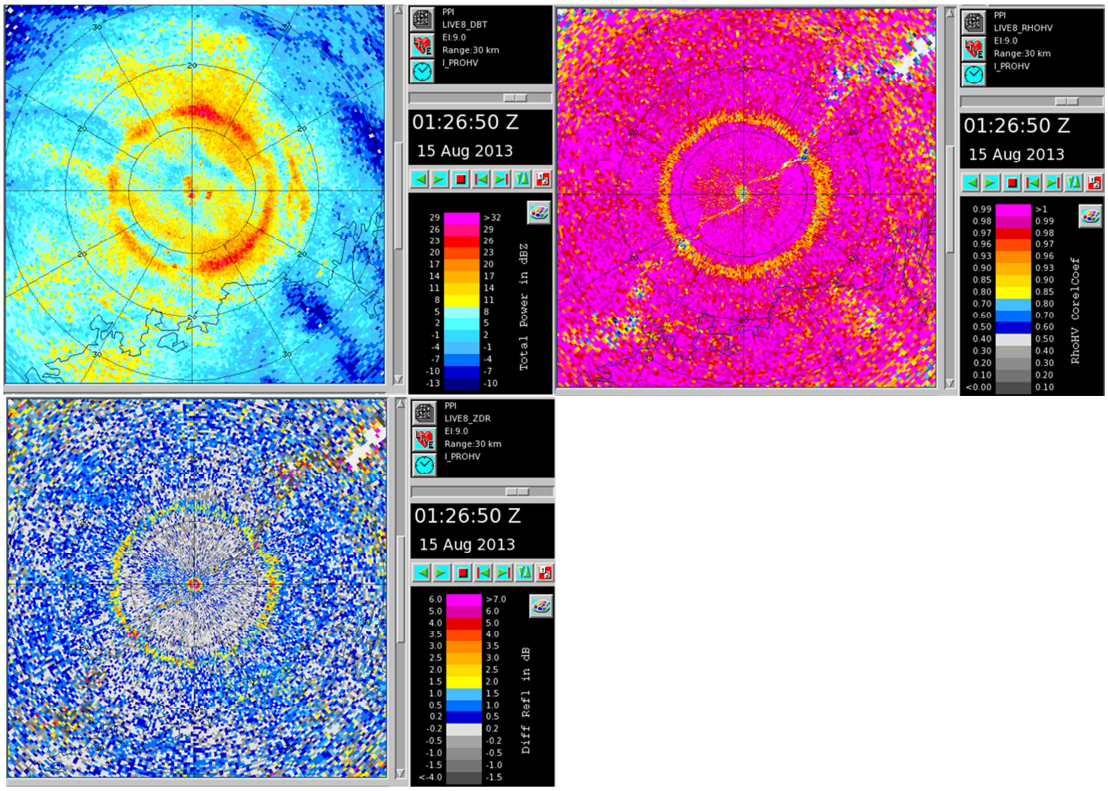

Figure 1 : Example of bright band signatures in C-band dual-polarization Doppler weather radar. Top left: reflectivity, top right: magnitude of the correlation coefficient between H and V channel echo, bottom left: differential reflectivity. The data are acquired by the Kerava radar, described in Section 4.

2.1 Methods of melting layer detection and estimation

Radar based methods of ML detection and estimation are conceptually considerations of bright band signals and their interpretation in terms of modelled ML parameters. The methodology is closely related with the broad research on and applications of vertical profiles of precipitation. We brief out just some analyses considering inputs from different types of observations. The methods aim at a variety of purposes such as direct hydrological interpretation of the bright band bottom, evaluation of the generality and of the intrinsic accuracy of radar based estimates, applications of vertical profile corrections, estimation of the large scale freezing level or recognition the bright band boundaries in specific radar sweep projections.

White et al. (2002) considered vertical profiles of echo and of Doppler vertical velocities observed in a network of wind profilers in the PACJET campaign. They estimate hourly altitudes of the bright band bottom from the negatively correlated gradients in the range corrected signal-to-noise ratio and in the vertical Doppler velocity. The estimates correlate well with the melting levels obtained from co-located concurrent rawinsonde profiles with an off-set of about 200 m which characterizes the ML thickness in the synoptic conditions of the land-falling winter storms at the Pacific West Coast.

Brandes and Ikeda (2004) considered the observations from a S-band dual-polarization Doppler radar (S-Pol) operated in the mode of alternated transmission in H and V polarization planes. Data were accumulated from several field programs conducted in different climate regions and seasons. Data allowed modelling independent profiles of reflectivity, of linear depolarization ratio (*LDR)* and of the magnitude of cross-correlation coefficient which are deemed representative of operational radar observations at ranges of less than 60 km. The freezing level is a parameter of the profile models. Comparisons with air-borne in-situ measurements of temperature indicated that the freezing levels can be estimated from the consensus estimates of remote radar observations at the spatial resolution of 5x5 km^2 and at accuracy of the order of 100 m, at radar ranges less than 60 km.

Zafar and Chandrasekar (2005) analysed the data from a full year of operations of the TRMM space-born radar using a self-organizing map. They conclude that the average profiles of reflectivity in stratiform precipitation are the same, globally. Tabary et al (2006) utilized the information in the co-polar correlation coefficient alone, for the purpose of estimating freezing levels taken constant within the radar range for operational uses. Matrosov et al. (2007) determined the melting layer boundaries and the freezing levels on a beam-by-beam basis by using ρ_{hv} and pronounced brightness in reflectivity.

Giangrande et al. (2008) proposed an automated melting layer detection algorithm which estimates the top and bottom of the melting layer considering Z, Z_{dr} and ρ_{hv} at elevation angles between 4 and 10 degrees for the specific operational use case at NEXRAD. The method assumes horizontal homogeneity of ML and it is limited to modest ranges due to stringent selection of elevations. These limitations have been refined in subsequent developments by Krause et al. (2013) which integrate radar observations with external information of wet bulb temperatures from rapidly updated numerical models. Recently, Frech et al. (2014) implemented an operational fuzzy logic hydrometeor classification in which the melting layer is a class. The information is used to give a better understanding of the meteorological conditions and improve the quantitative precipitation estimation.

3 Bayesian inference of MLHGT from fuzzy classifications of melting snow

We can describe the MLHGT estimation method as a stepwise procedure. A general flow diagram of the procedure is displayed in Figure 2. The procedure is repeated for each radar volume scan which can be either a collection of PPI or RHI sweeps. Observations from different radars are considered as independent data streams, which allow parallel processing of observations from an arbitrary number of radars in a network. Compositing can be envisaged as a step in which the MLHGT products of individual sites are merged by general purpose networking tools, for example by the criterion of highest radar confidence.

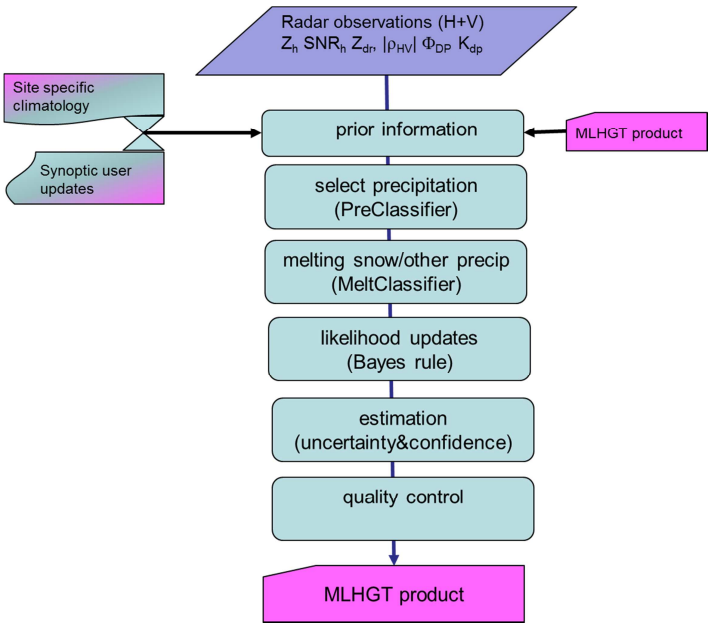

Figure 2: The flow diagram of the MLHGT procedure. The top level illustrates the radar observation inputs, followed by the origins of prior information. The blocks in the column illustrate the consecutive functional steps. A key qualifier of each step is expressed in parenthesis. At end, the procedure outputs a new MLHGT product file, for application uses and retrieved as a prior input in the next instance of the procedure.

3.1 Prior information in the MLHGT method

The MLHGT procedure considers *prior information* which may consist of the previous MLHGT product if available, and of the site specific average 0^oC isotherm. The mean 0^oC isotherm first specifies the center point of the interval in which the MLHGT estimates are allowed to vary, freely. We introduce a configurable parameter of **maximum variability** which characterizes the realistic limits of local climatology. The 0^oC isotherm parameter is retrieved from the metadata formatted in the radar observations at the radar. The setting may originate from the monthly climatology configured to each radar site, or it may originate from external information that is regularly uploaded to the radar.

The asymptotic value of MLHGT estimates in conditions of fair weather is the second use of the site specific 0^oC isotherm. As confidence decreases on radar observations, either due to their weakness or due to their latency in time, the MLHGT estimates approach smoothly to the values of 0^oC isotherm. We introduce a configurable parameter of **correlation time** which transforms the confidences of the radar based estimates derived in the recent past to the current moment in time. The correlation time characterizes the temporal variability of the weather in the local climatology. A typical parameter setting is of the order of one hour. The MLHGT procedure considers the **ML thickness** as a configurable constant.

3.2 Radar observations used in the MLHGT method

The MLHGT procedure considers selected subsets of precipitation signal which can be classified either as 'melting snow' or 'other precipitation' at a prescribed probability of correct classification and of false misinterpretation. The precipitation signals are computed from Doppler filtered moments acquired in the STAR mode. The fields of signal-to-noise (SNR_h), horizontal reflectivity, and differential reflectivity as well as the magnitude and the phase of co-polar correlation are considered. These measurands are subject to censoring on SNR_h and of ground clutter-to-signal ratio, applied in the common data stream of radar signal and data processing. Similarly, the common quality algorithms of the RVP900™ signal processor (Vaisala/Sigmet, 2013) are utilized. As known, operational radar echo often originates from other moving sources than precipitation and these 'non-meteorological' echo may dominate Doppler filtered data after common quality considerations. We utilize the HydroClass™ PreClassifier (Keränen et al, 2007) which recognizes the gates of non-meteorological echo to be omitted. PreClassifier originates from the JPOLE field experiment (Ryzhkov et al., 2005) while its fuzzy settings have been subsequently evolved based on the accumulated experience with Vaisala WRM200 radars in multiple climates and operational environments. The settings are common with other classifiers of HydroClass™.

3.3 Recognition of melting snow

We have constructed a dedicated fuzzy classifier 'MeltClassifier' in HydroClass™ for the purpose of radar based recognition of the locations of melting snow as well as of the locations where melting snow can be excluded. The recognition is purely based on radar observations i.e. no external information about ML is used in this step. MeltClassifier inherits the interpretation of hydrometeor signals parameterized in 'MeteoClassifier' (Lim et al, 2005) of HydroClass™. The binary MeltClassifier is constructed for stable performance such that the parameters of correct classifications and false misinterpretations can be estimated as internal constants of the MLHGT method. For these purposes, the MeteoClassifier membership functions of ML altitudes are replaced by those of SNR, and they are configured to consider signals strong enough for negligible impacts of thermal noise. The internal classes of MeteoClassifier other than 'melting snow' are re-grouped into the class of 'other precipitation', while the class of 'melting snow' remains as the complement. The fuzzy settings of the 'MeltClassifier' are managed analogously to other classifiers in HydroClass™.

3.4 The co-ordinate systems of the MLHGT method

The MLHGT method maps the locations of recognized 'melting snow' and 'other precipitation' into likelihood functions computed in the internal two-dimensional map of vertical columns. The columns are broad enough in azimuth and in range to collect sufficient statistics of entries from the volume scan data. The method thus uses the approach of Brandes and Ikeda (2004) which considered a grid of Earth co-ordinates within 60 km range from the radar. As known, the atmospheric ML is driven by the general advection and dynamics of atmosphere for which an Earth co-ordinate system is more appropriate than a radar centric view point. The latter is better suited for modeling the changes in radar capabilities as function of range, which needs to be accounted for when mapping the observations into MLHGT likelihoods. We introduce a configurable parameter for the **base spatial resolution** in number of sectors in azimuth, which is interpreted in characterizing the likelihood columns adjusted to be roughly the same size in azimuth and in range. We also allow the **vertical binning** of the likelihood functions to be configurable, and these two grid parameters are relevant for the availability of radar based MLHGT estimates, in combination with the correlation time parameter. By specifying a small base scale of the grid or a dense vertical binning, a higher total number of selected MeltClassifier estimates are needed as input for a given radar confidence level, which can realized at high availability for wide precipitation well covered by multiple radar data sweeps.

By specifying a modest scale of spatial resolution and vertical binning, data availability is optimized. In both cases, the actual spatial resolution varies as function of range from the radar.

By this construction, the method is able to recognize details of the MLHGT fields at ranges of tens of kilometers, while independent MLHGT estimates can be obtained up to distances beyond 100 km in conditions where sufficient amount of samples are obtained from precipitation recognized as 'melting snow' or as 'other precipitation'. We consider it important that MLHGT estimates may vary as function of range as a more realistic description of weather fronts, for example.

By construction, the MLHGT procedure does not impose strict requirements on the sweep geometry. For example, it can consider individual sweeps in RHI and in PPI, however with a significant trade-off in spatial resolution and coverage. Stable accuracy and good resolution are obtained when the volume scans sample the atmosphere at all the potential heights of ML.

3.5 Bayesian inference

Given these preparations with the radar observations of 'melting snow' and of 'other precipitation' and with the grid of vertical columns, the likelihoods of MLHGT can be updated in the Bayesian approach, for each radar observation (i.e. a bin recognized as 'melting snow' or 'other precipitation' by MeltClassifier). The Bayesian inference can be conceptually understood as mapping that is equivalent to constructing a display of vertical cross-section in which the most likely position of ML can be recognized by visual inspection of the MeltClassifier decisions.

3.6 Estimation of ML altitudes, of their uncertainties and of radar confidences

Upon completion of the volume data set, the end states of the likelihood functions are converted into estimates of MLHGT accompanied by the estimates of their uncertainty and confidence. In each vertical column, an MLHGT estimate is obtained as median of the values of the likelihood function. The uncertainty is estimated as the average of the 16^{th} upper and lower percentiles of the likelihood function ("one-sigma" error in Gaussian interpretation). The radar confidences are combined from the shape of the resulting likelihood function and from the number of Bayesian updates (i.e. number of MeltClassifier entries) of which the latter is typically the deciding factor, as explained next.

In the limit of very high statistics while a low probability of correct classifications as well as low rate of misclassifications, radar confidence can be defined as the fraction of 'radar based information' in the likelihood function. In absence of any radar information, the MLHGT likelihood function is uniform in interval allowed by climatology and it vanishes elsewhere. In uniform likelihood, the radar based confidence is zero. Radar information accumulates into a peak which gradually grows corresponding to the growth in radar based confidence, while the initially flat background is suppressed due to normalization to unity. Eventually, the likelihood function is concentrated in the peak which has the width corresponding to the uncertainty in MLHGT. The maximal radar confidence of unity corresponds to a vanishing flat background. The radar confidence can be formally defined as the integral of the MLHGT likelihood function in the peak of radar based information, which is the complement of the integral of the flat component of the likelihood function. In practice, MeltClassifier is configured to a fair probability of correct classifications and a finite number of observations are sufficient for MLHGT estimates of a high radar confidence. The features of randomness in the finite number of entries are the limiting factor in judging the confidence of 'peaks'. The variances of the peak confidences are a function of number of entries and of the probability of correct classifications as well as rate of misclassifications. This relation is parameterized in the MLHGT method through numerical simulations of the repeated updates of the Bayesian rule.

3.7 Quality control and MLHGT product output

At each internal grid point, the procedure may check the consistency of radar confidence by comparing it with those in the neighboring grid points. The confidence is accepted if it exceeds a **minimum confidence level and** a configurable **minimum number of grid neighbors** meet the minimum confidence level, else the confidence is set to a very low value.

The MLHGT product is formatted as an independently configurable grid of configurable system of Earth co-ordinates. T**he maximum range** and **the output resolution** of the MLHGT product are technical parameters of this step. The product consists of three fields: the MLHGT estimates, their uncertainties and their radar confidences. The data in the output grid are filled by values interpolated from the internal grid of MLHGT estimates, of their uncertainties and of radar confidences. The MLHGT product file includes headers of metadata describing the methods settings and of the relevant metadata inherited from the radar observations used as input, following the conventions of the public IRIS™ data format (IRIS, 2014).

4 Data examples and validation

4.1 Instruments and measurements

The MLHGT estimates were validated by considering the observations from two proximately located C-band polarimetric weather radars with comparison to in-site measurements in upper air soundings. Figure 3 shows the locations of the radar sites and of the two sounding stations considered. Vaisala operates a C-band dual-polarization Doppler weather radar (WRM200) located on the top of a water tower in the town of Kerava. Table 1 shows the parameters of the magnetron weather radar system. University of Helsinki operates a C-band dual-polarization Doppler weather radar (WRK200) at Kumpula campus. The parameters of the klystron weather radar system are those of WRM200 (Table 1), except the klystron power amplifier which is used in generating the transmitted RF pulses.

Upper air soundings are carried daily at 00 UTC and 12 UTC at the WMO site of Jokioinen, located at roughly 106 km northwest from the Kerava radar. Quality soundings are launched, typically on working days, at Vaisala headquarters, located in Vantaa at approximately 20 km southwest from the Kerava radar. The weather events have been continuously monitored at University of Helsinki Kumpula (Leskinen, 2014), through archival of the radar observations, of various surface observations including measurements of temperature. This background information is utilized in selecting the precipitation events to be considered in validation.

The Kerava radar observations consist of volume scans repeated every fifteen minutes. The pulse length of 2 µs is used at the pulse repetition frequency of 570 Hz. The maximum range is 250 km. Data are acquired in the STAR mode at seven elevations of 0.5, 1.5, 2.5, 4.5 7.0, 10.5 and 15.0 degrees. Doppler filtered moment data are computed from 32 pulses at the base gate spacing of 250 m. Moment data are summed form two consecutive gates ending up with the spatial resolution of 500 m. The Kumpula radar observations consist of range-height (RHI) scans from the elevation of 0 degrees up to 20 degrees made towards the Kerava radar in the northeast (radar azimuth of 11.8 degrees). Kumpula data are acquired at the pulse width 0.5 µs with gate spacing of 50 m up to the range of 50km. The moment data are computed from 256 samples.

The radar specific settings of the mean 0^{o}C isotherm are interpolated from the temperature profiles of the upper air soundings carried out at the nearest WMO meteorological stations of Jokioinen and of Tallin, roughly 130 km southwest from the Kerava radar. The settings are updated to the radars daily at 1 UTC.

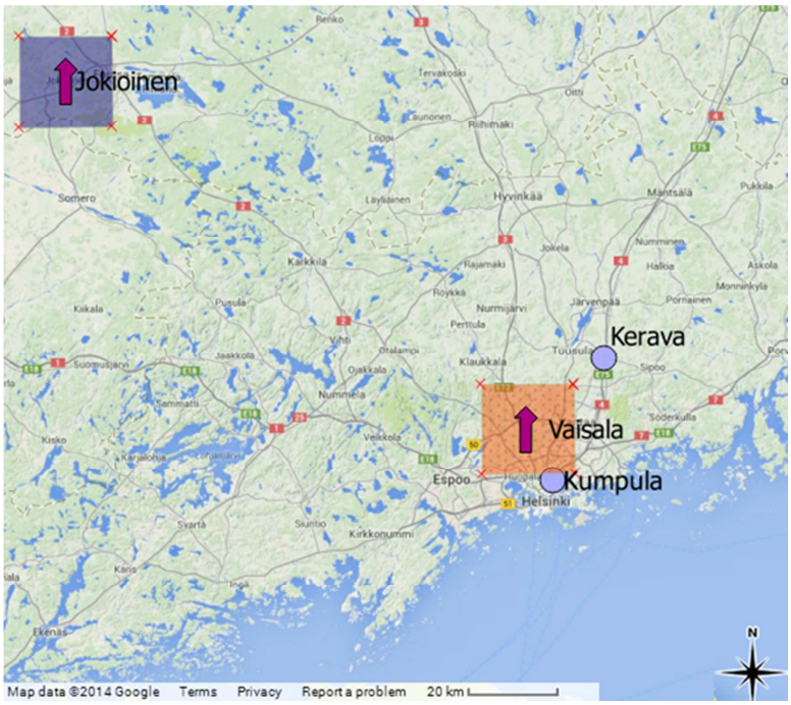

Figure 3: Measurement area and sites considered in the validation. Light purple circles: the WRM200 radar at Kerava and the WRK200 radar at Kumpula campus of University of Helsinki. Purple arrows: the sounding launch sites at Vaisala (~20 km from the Kerava radar) and the WMO site of Jokioinen (~100 km from the Kerava radar). The purple and orange squares indicate the areas of 20 x 20 km^2 around the sounding launch sites, in which MLHGT estimates are validated.

4.2 Data Examples

We consider the evolution of the weather on the morning hours of June 20th 2013 when a broad system of precipitation approached from southwest. At midnight, the temperature profile from the synoptic upper air sounding indicates the momentary freezing level was 3200 +/- 50 m at Tallinn some 120 km southwest from the Kerava radar. At the WMO site of Jokioinen about 100 km west from Kerava, it was at the level of 2950 +/- 50 m at midnight while it was at the level of 3400 /- 50 m at noon. We consider these air masses are warm in the season. The values at midnight were interpolated into the Kerava radar specific 0°C isotherm value of 3100 m at 01UTC.

Table 1: Parameters of the WRM200 dual-polarization Doppler weather radar

Transmitter		***Antenna***	
Tyype	Magnetron	*Reflector type*	Center fed parabolic
Operating frequency	5.5-5.7 Ghz	*Diameter*	4.5 m
Peak power	250kW	*Gain (typical)*	45 dB
Pulse width	0.5, 0.8, 1.0, 2.0 µs	*Beam width*	<1 degree
PRF	200 to 2400 Hz	*Side lobes*	-33 dB (typical, on axis)
RF-to-IF receiver		***Pedestal***	
IF downconversion	Dual stage, dual channel	*Type*	Semi yoke elevation over azimuth
Dynamic range	>99dB (2 µs pulse)	*Elevation range*	-2 to 108 degrees
IF frequency	442/60 MHz	*Max. scan rate*	40 deg/sec
Noise figure	< 2 dB	*Position accuracy*	Better than 0.1 deg
Digital receiver, signal processor, data processing			
Signal processor type		VAISALA SIGMET RVP900™ / IRIS™	
IF digitizer		16 bits, 100 MHz in 5 channels	

The method was configured to vary MLHGT by +/- 2000 m around the site mean freezing level. The correlation time was set to three hours. The base resolution scale was set to correspond a grid 20x20 km^2 for MLHGT estimates at the range of 50 km from the radar. The ML thickness was modelled to 500 m. The first MLHGT estimates of 2700-2800 m were obtained as soon as significant precipitation reached the distance of 120 km, observed at 03:23UTC at the lowest elevation of 0.5° in use. The first significant variability in ML altitudes from 1600 m to 3400 m was evident at 03:53UTC as illustrated in Figure 4.

The observations display a persistent pattern of cold air band associated with the front edge of precipitation propagating into northeast. The pattern can be inferred from the signatures of bright band which normally (constant level of ML) form a ring shape, while in this event the signature is stretched into a curved surface oriented in the direction from northwest into southeast. The particular pattern is visible in the lowest elevation data and it is confirmed when all the elevations are inspected. The data acquired at 05:08UTC is illustrated in Figure 5. It displays distinct regions of melting layer stretching into the direction of the azimuth of 300 degrees with another narrow ML band at the azimuth of 340 degrees, approximately. The pattern is repeated at higher elevations which lead to the conclusion that the region marked in the reflectivity field is filled by frozen hydrometeors above ML, while the echo at the same range but in the direction of southwest is likely rain below ML. The nontrivial surface of ML is consistently reconstructed by the MLHGT method, in regions of high radar confidence. The band of freezing air reached altitudes as low as 1600 m. The band is followed by a region of warm air in which the MLHGT estimates stabilize at the level of 3300-3400 m, inferred from radar observations which accumulate to a non-vanishing radar confidence level above -20 dB.

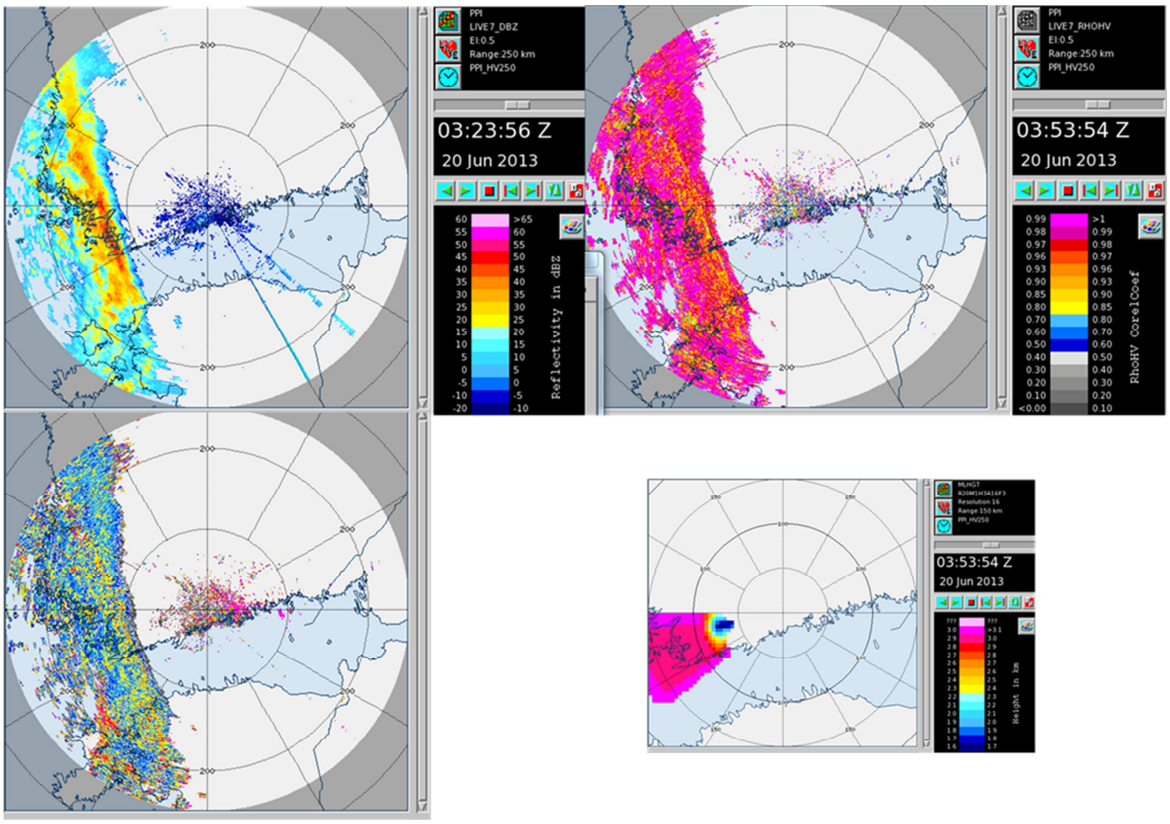

Figure 4: Frontal system of precipitation approaching the Kerava WRM200 radar from southwest, at the moment when the estimates indicate first significant variability in MLHGT. Top left: reflectivity, top right: $|\rho_{hv}|$, bottom left: differential reflectivity at the elevation of 0.5 degrees. Bottom right: map of the MLHGT estimates displayed for radar confidences higher than -20 dB. The size of the MLHGT product display is scaled to match with the maximum range of 250 km in the other data displays.

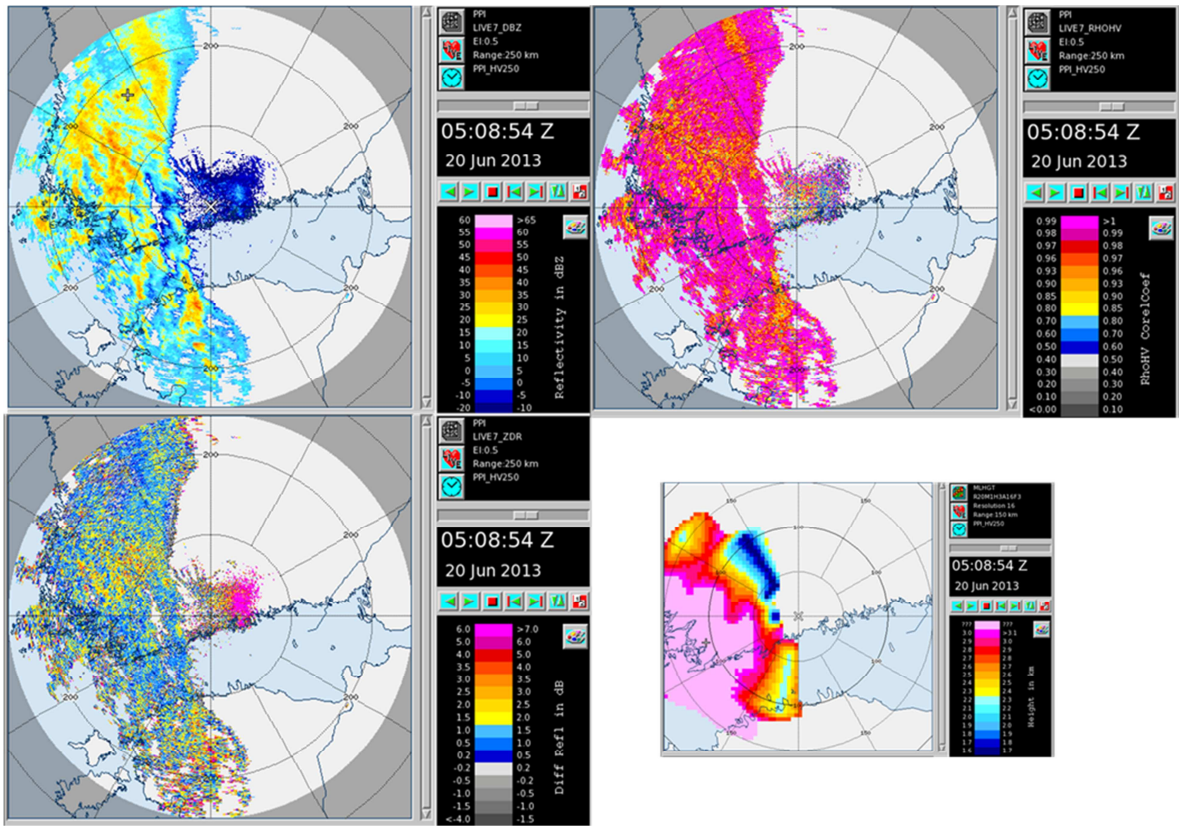

Figure 5: As Figure 4, but about two hours later when the precipitation at surface reached the distance of about 50 km from to the radar. The marker in the display of reflectivity is at the range of 170 km at the altitude of 3300 m in the region of cold air implying MLHGT values well below 2 km. The echo likely originates from frozen hydrometeors, while the echoes at the same ranges into west are likely originate from ML estimated to exist at the height above 3 km. The marker in the MLHGT map indicates the highest estimate of 3400 m.

At 07UTC, precipitation reached the radar sites at Kumpula and Kerava allowing detailed maps of MLHGT estimates to be obtained from both radars, independently. At that moment, the weather was evolved from the compact front of precipitation into a set of local showers passing through the Helsinki area. Figure 6 displays the observations of the Kerava radar 06:54 UTC, as well as the MLHGT estimates. The data at elevation of 1.5 degrees display a clear ML pattern at distances within 100 km from the radar. However, the usual ring pattern is tilted indicating a strong local gradient in ML. Indeed, such a gradient is reconstructed by the MLHGT method. The MLHGT estimates range from 3000 m down to 1900 m and the field indicates a general gradient in excess of 1000 m in about 50 km.

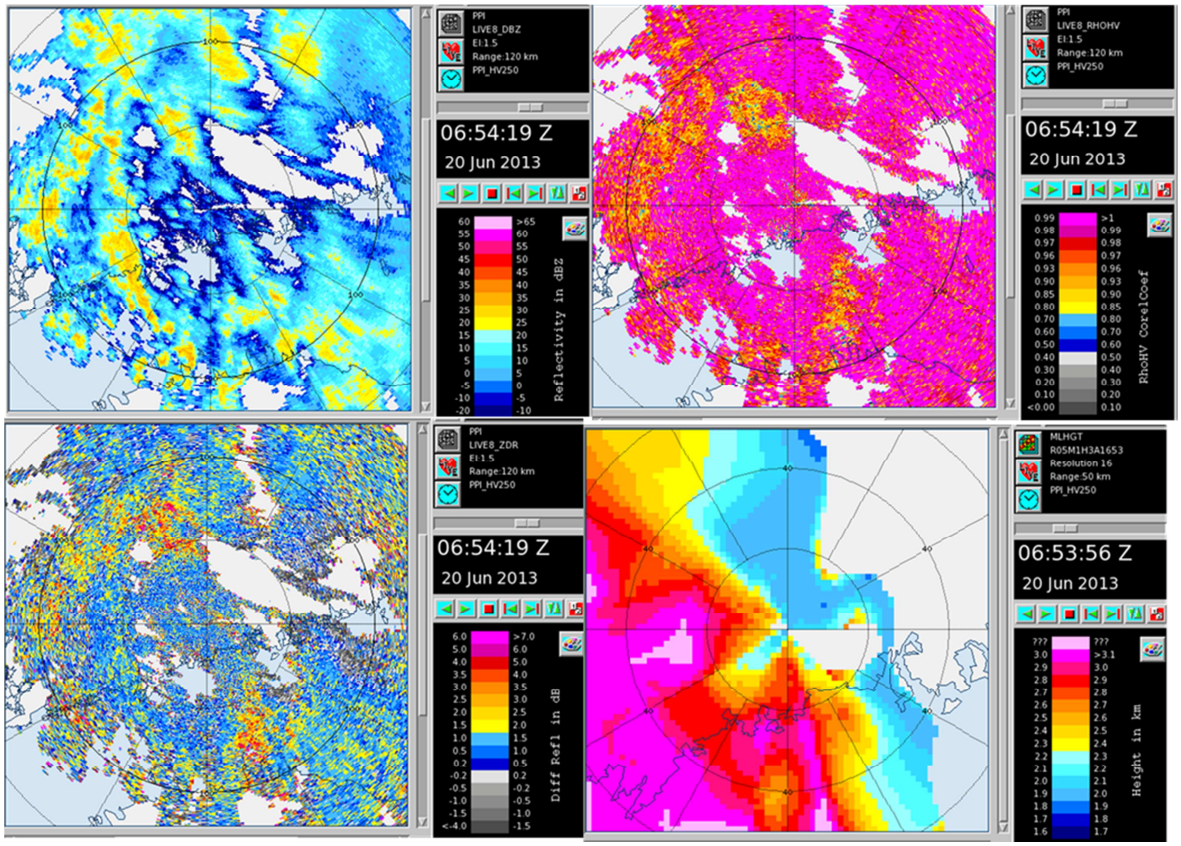

Figure 6: As Figure 4, but three hours later when the band of cold air was just passing the Kerava radar. Data are exceptionally at the elevation of 1.5 degrees up to ranges of 120 km, and they display the tilted pattern of the bright band, unambiguously. The MLHGT estimates are displayed for radar confidences higher than -5 dB in a product computed up to the range of 50 km.

The observations of the Kerava radar can be compared with the nearly co-incident observations of the Kumpula radar which is observing in the direction of Kerava. As shown in Figure 6, the bright band is unambiguously seen in the RHI scan. Furthermore, the significant gradient in MLHGT of about 1000 m in 50 km is confirmed. The MLHGT estimates reconstructed from the Kumpula radar RHI sweep data agree very well with the values obtained in the same locations from the independent observations of the Kerava radar, see Figure 7.

4.3 Validation of the MLHGT estimates with respect to 0^{o}C isotherms from upper air soundings

Observations of Kerava WRM200 and Kumpula WRK200 weather radars have been processed with the MLHGT method in substantial intervals starting from June 2013 to summer 2014. A week in June 2013 with precipitation in summer conditions and another week of precipitation in the cool season in November 2013 were selected for detailed validation of the MLGHT estimates through comparison with 0^{o}C isotherms derived from the profiles of the upper air sounding data. The sounding data are referenced to the location and the time at the launch, while the relevant measurements of temperature are made several minutes later at a location drifted from the launch site. Similarly, the radar scan time of the volume data spans through several minutes, repeated for every 15 minutes. Conservatively, the MLHGT estimates were considered in the area of 20x20 km^2 around the launch location. The values of MLHGT estimates were averaged into a single estimate at the time of the radar volume time.

.

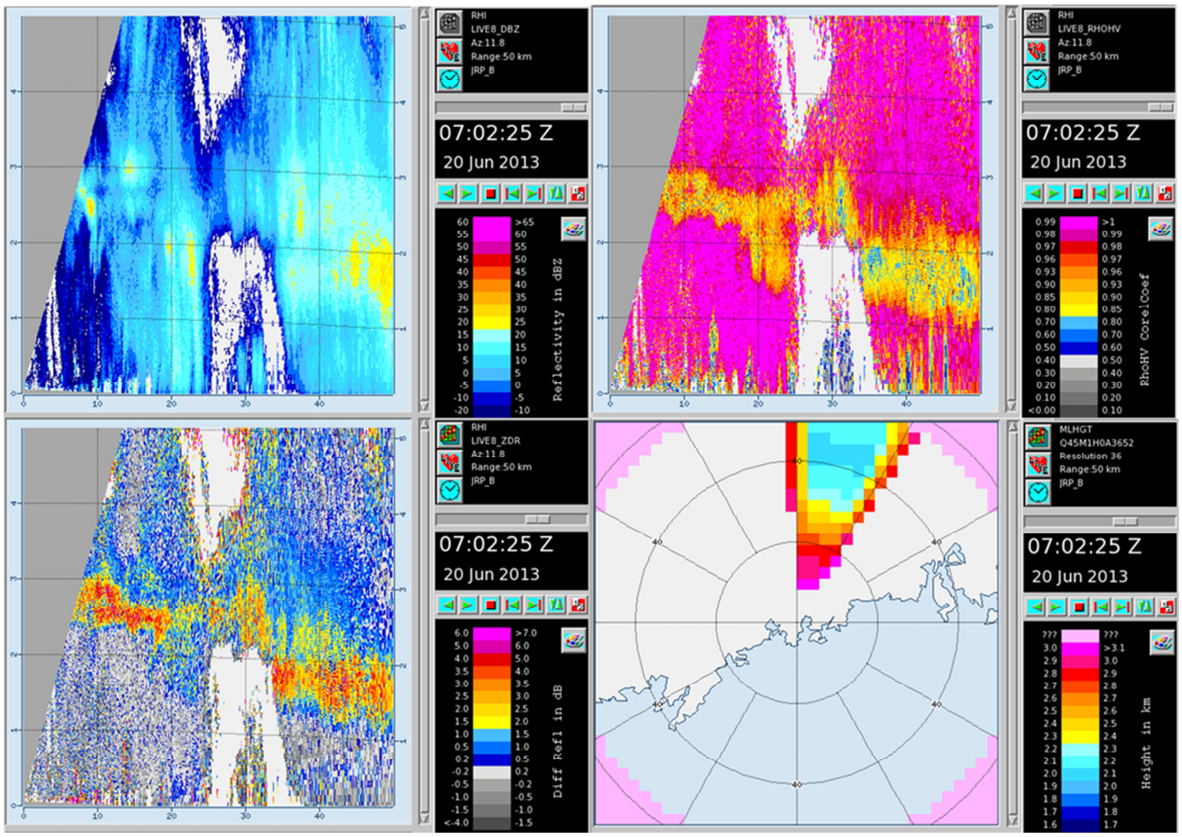

Figure 7: Observations from a range-height sweep (RHI) acquired at the Kumpula WRK200 radar into the direction of the Kerava radar. at the moment when the band of cold air mass is passing the Helsinki region. Top left: Doppler reflectivity, top right: co-polar correlation coefficient, bottom left: differential reflectivity and bottom right: map of the MLHGT estimates displayed for radar confidences higher than -35 dB. They are available in the sector of the RHI scan, used as input.

Conservatively, we allow ML to vary in the interval of 4000 m centered on the radar wide 0^{o}C isotherm. We select a correlation time of 3 hours. We select a resolution of 24 sectors in azimuth, which corresponds to the internal MLHGT spatial resolution of 5x5 km^2, approximately at the distance of Vaisala soundings (30 km). For evaluation purposes we consider and display the estimates at all the radar confidence levels. The thickness of the melting layer was modeled to be 500 m.

Figure 8 shows the time series of the estimated melting layer altitudes during the summer week from 12^{th} to 20^{th} of June 2013 at the location of Vaisala soundings (~20km from the radar). In the top panel, the green data points are MLHGT estimates obtained from the Kerava WRM200 observations at radar confidences levels greater that -20dB, while the blue data points are lower radar confidence data (intervals of fair weather). Each radar data point is associated with the estimate of one-sigma uncertainty. The red data points represent the 0^{o}C isotherms derived from Vaisala soundings, which indicate variability of freezing levels in the interval from 1900 m to 3100 m. The vertical scale of the graph is approximately the span where MLHGT estimates are allowed to vary, freely. The absence of radar data form 12^{th} to 14^{th} and from 18^{th} to 19^{th} of June corresponds to pauses on the operation of the radar due to maintenance or programed visits.

We observe trends in radar based estimates which are highly consistent with the broad conditions of the atmosphere as captured by the sounding data. The radar confidences correctly characterize the availability of precipitation signals. In the intervals of fair weather the radar confidences decrease and the MLHGT estimates approach to the radar site specific 0^{o}C isotherms. The intervals of high radar confidence correspond to the conditions of precipitation at the evaluated location. We observe significant variability in radar based estimates which however coincide with the momentary estimates of 0^{o}C isotherms obtained from independent sounding data. The agreement is at the level of 100 m. The estimates of uncertainty are of the same magnitude. The complexity of atmosphere is illustrated in the moment of last sounding, June 20^{th} where the temperature profiles suggest for two levels of 0^{o}C isotherms, out of which the lower one is accurately estimated as MLHGT by the radar based method.

Figure 9 shows the time series of the estimated melting layer altitudes in the same time interval but at the WMO site of Jokioinen (~106 km from the radar). Due to the larger distance, the radar confidences are generally lower and availability of high confidence radar estimates tends to be reduced. In order to compensate this, the spatial base scale was increased to 16 sectors, corresponding to the spatial resolution of 40x40 km^2 at the distance of Jokioinen. The vertical bin size was slightly increased to 300 m. With these settings, the availability of MLHGT estimates is good for reasonable radar confidences above -10 dB, up to the distances of 100 km in conditions in which the echo tops reach altitudes of several kilometers. Indeed,

MLHGT estimates are obtained in the warm events in the time interval and the values agree very well with the in-situ observations of the sounding data. In particular at noon June 16th, the radar based observations correctly recognize the freezing level which is significantly lower than the extrapolation from synoptic observations made 12 hours earlier. The data related with the event of large frontal system approaching from southwest in the morning of June 20th is considered in the previous Section.

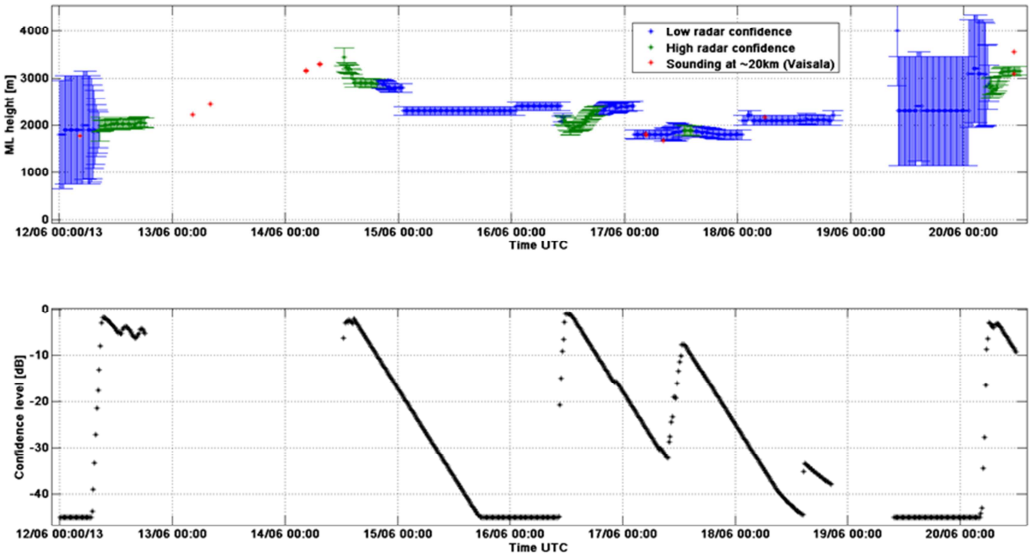

Figure 8: Top: MLHGT estimates of melting layer altitudes and associated one-sigma uncertainties in the time interval from June 12th to June 20th, 2013. The green points relate with high radar confidences greater than -10 dB and (blue) radar confidences lower than -10 dB. Red points are the 0°C isotherms derived from the temperature profiles of upper air soundings carried at Vaisala. Bottom: The levels of radar confidences corresponding to the MLHGT estimates in top. The radar was not in operation in the interval starting from the evening June 12th and in the short interval in the evening June 19th.

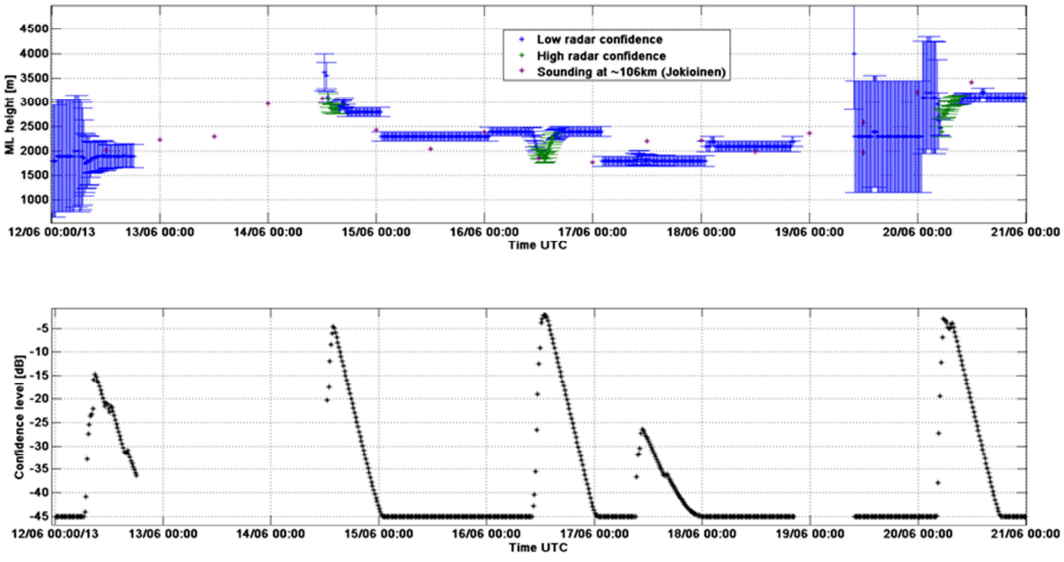

Figure 9: As Figure 8 but for the location of Jokioinen at the distance of 106 km from the Kerava radar.

Figure 10 shows the time series of the estimates of the melting layer altitudes during the cool season week from 20th to 28th November 2013 at the Vaisala sounding launching area (~20 km from the radar) estimated using Kerava radar observations. The Kerava radar was operating continuously. The sounding data indicate the freezing levels varied from surface (at approximately 50 MSL) up to altitudes of 1000 m. Precipitation persisted through intervals of days during which

the radar confidences kept at a high level. In those intervals, the MLHGT estimates vary by more than 1000 m, while they coincide quite accurately with the momentary values of 0°C isotherms derived from independent temperature profiles of soundings. On the November 27th, sounding data suggests for a moment of multiple levels of 0°C isotherms separated by some 500 m, confirmed by two soundings carried out within an hour. At that moment, MLHGT estimates are lacking precipitation signals while the method reports a value close to the lower level, with an excess in uncertainty of a few hundred meters.

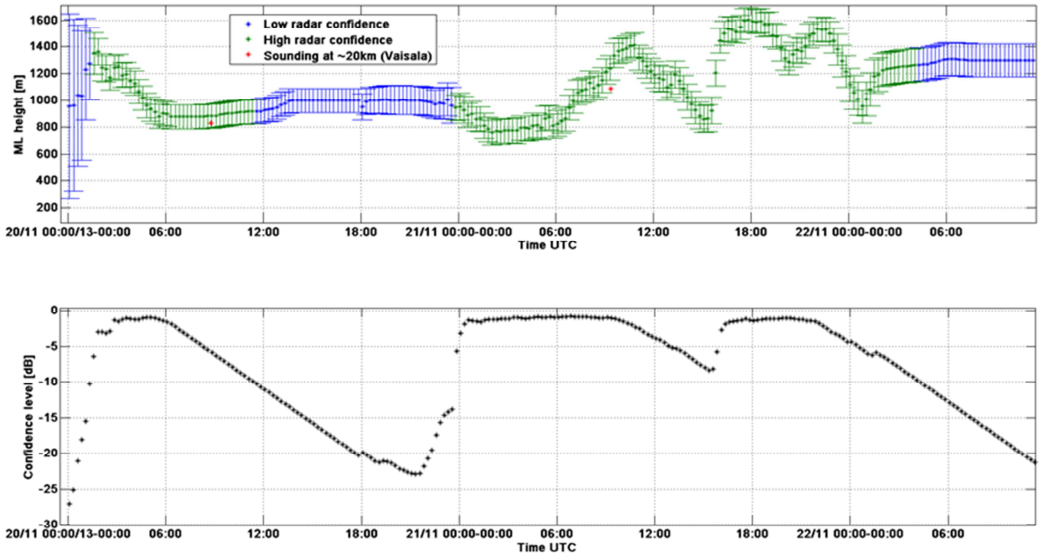

Figure 10: As Figure 8, but for the sub-interval of time period from November 20th to November 22th, 2013.

5 Summary and discussion

We have developed and implemented a method for estimating melting layer altitudes from observations of dual-polarization Doppler weather radar. The method is designed for near-real-time operational uses and applications. In a robust and consistent manner, the radar description of melting layer is expanded from the first order parameterization of site specific climatology of semi static 0°C isotherms into high resolution maps of spatially variable melting layer altitudes evolving in time. Using a Bayesian approach, the method accumulates locations of recognized (and excluded) melting snow into a grid of likelihoods from which the altitudes of the melting layer can be estimated at a high spatial and temporal resolution. The method provides with the estimates of uncertainty and with the confidences of the radar information. The method is configurable with a few parameters. The method can consider both PPI and RHI type of volumes scan data, acquired in the STAR mode of dual-polarization weather radar.

The MLHGT estimates are able to map evolution of the melting layer as a function of range up to distances of 100 km, in frequently occurring warm season conditions. This is an important capability in events of frontal systems with large and rapid changes in the freezing level. In favorable conditions and settings, the method provides reliable estimates of melting layer close to ground. By conception, it is able to deduce freezing precipitation at surface through exclusion of the melting layer. These are potential inputs to radar based estimates of surface precipitation type.

The estimated melting layer altitudes are reported in a map in Earth coordinates in as a standard Cartesian MLHGT product in the IRIS™ radar data format. The method can be scheduled to run at the radar computer, or it can be scheduled to process observations from radar networks routed to the central processing analysis facility, in near-real-time. The product information can be promptly uploaded to the radar RVP900™ signal processor for utilization in the real-time methods of hydrometeor identification as well as in the dual-polarization corrections for rain induced attenuation. The product format is public and allows wider uses or even updates of the MLHGT estimates in applications.

The MLHGT method has been evaluated in conditions of warm and cool season, with direct validation with respect to independent upper air soundings. The MLHGT estimates, the estimates of their uncertainty and of radar confidence are found to perform consistently. In first validations covering about a dozen co-incidences of upper air soundings and MLHGT estimates at high radar confidence (precipitation signals available), the remote MLHGT estimates and the 0°C isotherms derived from in-situ temperature profiles are found to agree at the level of 100 m.

References

Fabry, F. and Zawadzki, I. Long Term Radar Observations of the Melting Layer and Precipitation and Their Interpretation // Journal of the atmospheric Sciences. -April 1995.- 7: Vol. 52.-pp. 838-851.

Koistinen, J. and Pohjola, H. Estimation of Ground-Level reflectivity Factors in operational Weather Radar Networks Using VPR-Based correction Ensembles// Journal of Applied Meteorology and Climotology. - doi: http://dx.doi.org/10.1175/JAMC-D-13-0343.1.

White A. B, Gottas, D.J, Strem E.T, Ralph F.M. and Neiman P.J. An Automated Brightband Height Detection Algorithm for Use with Doppler Radar Spectral Moment // Journal of atmospheric and oceanic technology. -May 2002.- 1: Vol. 19.- pp. 687-697p.

Brandes, E.A and Ikeda, K. Freezing –Level Estimation with Polarimetric Radar // Journal of applied meteorology. - November 2004.- 1:Vol. 43.-pp. 1541-1553.

Zafar B. and Chandrasekar V. A Methodology to Study Bright Band Structure on a Global Scale from TRMM Precipitation Radar // IGARSS '05, Proceedings 2005 IEEE International, Vol. 5, pp. 3400-3403.

Tabary, P., Le Henaff A., Vulpiani G., Parent-du-Châtelet J. and Gourley J.J. Melting layer characterization and identification with a C-band dual-polarization radar: A long-term analysis // Preprints, Fourth European Conf. on Radar in Meteorology and Hydrology (ERAD 2006), Barcelona, Spain.

Matrosov S.Y. Clark K.A. and Kingsmill D.E. Polarimetric Radar Approach to Identify Rain, Melting-Layer, and Snow regions for applying Corrections to Vertical Profiles of Relectivity // Journal of applied meteorology and climatology - February 2007.- 1: Vol. 46. pp. 154 -166.

Giangrande, S.E., Krause, J. and Ryzhkov, A.V. Automatic Designation of the Melting Layer with a Polarimetric Prototype of the WSR-88D Radar // Journal of applied meteorology and climatology. - May 2008.- 1: Vol. 47.-pp. 1354 - 1364.

Krause J., **Lakshmanan V., Ryzhkov A.** Improving detection of the melting layer using dual-polarization radar, NWP model data, and object identification techniques // AMS 36th Conference on Radar Meteorology, September, 2013, Breckenridge, CO, USA. https://ams.confex.com/ams/36Radar/webprogram/Paper228651.html - Url visited 18.07.2014.

Vaisala/Sigmet RVP900™ Digital Receiver, User's Manual, 2013
http://www.vaisala.com/en/products/weatherradars/Pages/RVP900.aspx and
ftp://ftp.sigmet.com/outgoing/manuals/RVP900_Users_Manual.pdf - Url visited 16.07.2014.

Keränen R., Saltikoff E., Chandrasekar V. Lim S., Holmes J. and Selzler J. Real-time Hydrometeor Classification for the Operational Forecasting Environment, AMS 33rd Conference on Radar Meteorology, August 2007 - https://ams.confex.com/ams/33Radar/techprogram/paper_123476.htm - Url visited 13.07.2014.

Ryzhkov, A.V., Schuur, T.J., Burgess, D.W., Heinselman, P.L. Giangrande, S.E. and Zrnić, D.S. The Joint Polarization Experiment Polarimetric Rainfall Measurements and Hydrometeor Classification // Bulletin American Meteorological Society. -June 2005.- 1:Vol. 86.-pp. 809-824.

Lim, S., Chandrasekar V. and Bringi V.N., Hydrometeor classification system using dual polarization radar measurements: model improvements and in situ verification, 2005, *IEEE Trans. Geoscience and Remote Sensing*, **43**, 792-801p.

Frech, M. and Steinert, J. Polarimetric radar observations during an orographic rain event and the performance of a hydrometeor classification scheme // Journal Hydrology and Earth System Sciences (HES), July 2014.-Vol:11.-pp. 8845-8877

Vaisala/Sigmet IRIS™ Progammer's Manual, 2014
http://www.vaisala.com/en/products/weatherradars/Pages/IRIS.aspx and
ftp://ftp.sigmet.com/outgoing/manuals/IRIS_Programmers_Manual.pdf - Url visited 16.07.2014.

Leskinen, M. Meteorological data in graphs. http://www.atm.helsinki.fi/~mleskine/TESTBED/kumpula.html. July 2014. - Url visited 07.07.2014.

Helsinki University Radar Group. Observation sites: Instruments. http://www.atm.helsinki.fi/UH_RADAR/sites.html. December 2013. - Url visited 14.07.2014.

Vaisala Vaisala Weather Radar WRM200 http://www.vaisala.com/en/products/weatherradars/Pages/WRM200.aspx;
IRIS Weather Radar software http://www.vaisala.com/en/products/weatherradars/Pages/IRIS.aspx;
- Url visited 14.07.2014.